Supplementary Information for

Towards Highlighting the Ultrafast Electron Transfer Dynamics at the Optically-Dark Sites of Photocatalysts

Sophie E. Canton,[◊] Xiaoyi Zhang,[§*] Jianxin Zhang,[‡] Tim B. van Driel,[∫] Kasper S. Kjaer,[∬] Kristoffer Haldrup,[∫] Pavel Chabera,[#] Tobias Harlang,[#] Karina Suarez-Alcantara,[◊] Yizhu Liu,[‡] Jorge Pérez,[‡] Amélie Bordage,[%,¥] Mátyás Pápai,[%] György Vankó,[%] Guy Jennings,[§] Charles A. Kurtz,[§] Mauro Rovezzi,[&] Pieter Glatzel,[&] Grigory Smolentsev,[#] Jens Uhlig,[#] Asmus O. Dohn,[∬∫] Morten Christensen,[∫] Andreas Galler,[†] Wojciech Gawelda,[†] Christian Bressler,[†] Henrik T. Lemke,[$] Klaus B. Møller,[∬] Martin M. Nielsen,[∫] Reiner Lomoth,[||] Kenneth Wärnmark[‡] , and Villy Sundström [#]**

[◊] Department of Synchrotron Radiation Instrumentation, PO Box 118, Lund University, 22100 Lund, Sweden
[§] X-ray Sciences Division, Argonne National Laboratory, 9700 South Cass Avenue, Argonne, Illinois 60439, USA
[‡] Centre for Analysis and Synthesis, Department of Chemistry, Lund University, S-22100 Lund, Sweden
[∫] Centre for Molecular Movies, Department of Physics, Technical University of Denmark, DK-2800, Lyngby, Denmark
[∬] Centre for Molecular Movies, Niels Bohr Institute, University of Copenhagen, DK-2100, Copenhagen, Denmark
[#] Chemical Physics Department, PO Box 118, Lund University, S-22100 Lund, Sweden
[%] Wigner Research Centre for Physics, Hungarian Academy Sciences, H-1525 Budapest, P.O.B. 49, Hungary
[¥] Institut Néel, CNRS et Université Joseph Fourier, BP 166, F-38042 Grenoble Cedex 9, France
[&] European Synchrotron Radiation Facility, BP 220, F-38043 Grenoble, France
[∬∫] Department of Chemistry, Technical University of Denmark, DK-2800, Kgs. Lyngby, Denmark
[†] European XFEL Facility, Albert-Einstein Ring 19, D-22 761 Hamburg, Germany
[$] SLAC National l Accelerator Laboratory, Linac Coherent Light Source, Menlo Park, CA 94025 USA
|| Department of Chemistry-Ångström laboratory, Box 523, Uppsala University, S-75120 Uppsala, Sweden

S_1 Synthesis and characterization of $[(bpy)_2Ru^{II}(tpphz)^1Co^{III}(bpy)_2](PF_6)_5$.

General methods: All chemicals were used as received from commercial sources without further purification except for diethyl ether that was obtained from a dry solvent dispenser system (MBraun 7656). PE refers to petroleum ether (boiling range 40-60 °C). Precoated Merk silica gel 60 F_{254} plates were used for TLC analysis. NMR spectra were recorded on a Bruker Avance 400 NMR spectrometer. Chemical shifts (δ) are reported relative to shift-scale calibrated with the residual NMR solvent peak DMSO-d_6 (2.50 ppm for ^{1}H NMR). Elemental analyses were performed by Mikroanalytisches Laboratorium Kolbe (Germany).

cis-$[Co(bpy)_2Cl_2]Cl$.[1]

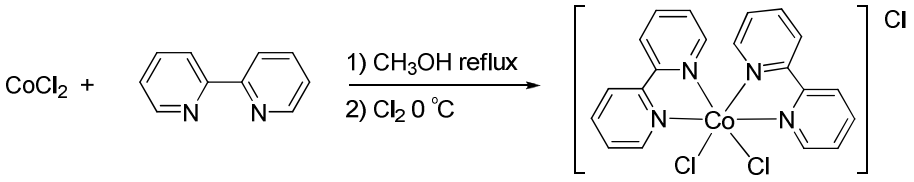

Procedure: A methanolic solution of 2,2'-dipyridyl (2.0 g, 12.8 mmol) was heated to reflux, then a methanolic solution of $CoCl_2$ (0.83 g, 8.4 mmol) was added. The solution was refluxed for 1 hour, after the solution was cooled with ice-bath and bubbled with Cl_2 gas until a gray precipitate was formed. The gray solid was collected and washed with diethyl ether and dried under vacuum, and 0.83 g (23%) of *cis*-$[Co(bpy)_2Cl_2]Cl$ was obtained.

cis-$[Co(bpy)_2(OTf)_2]OTf$.[2]

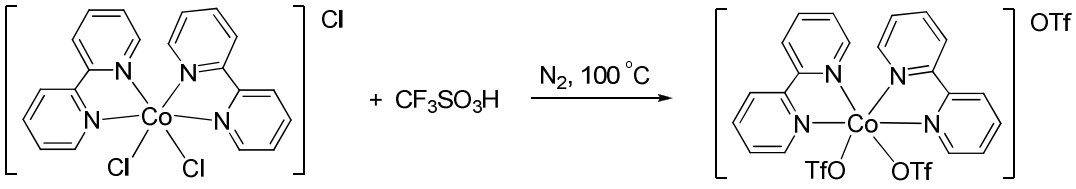

Procedure: In a 100 mL round-bottomed flask, (200 mg, 0.35 mmol) of *cis*-$[Co(bpy)_2Cl_2]Cl$ was dissolved in 3.5 mL CF_3SO_3H. The mixture was heated to 100 ℃ for 3 hours. After the mixture was cooled to room temperature 35 mL diethyl ether was added. The yellow solid was collected and washed with diethyl ether and dried under vacuum, and 230 mg (79%) of *cis*-$[Co(bpy)_2OTf_2]OTf$ was obtained.

$[Ru(bpy)_2tpphzCo(bpy)_2](PF_6)_5$.

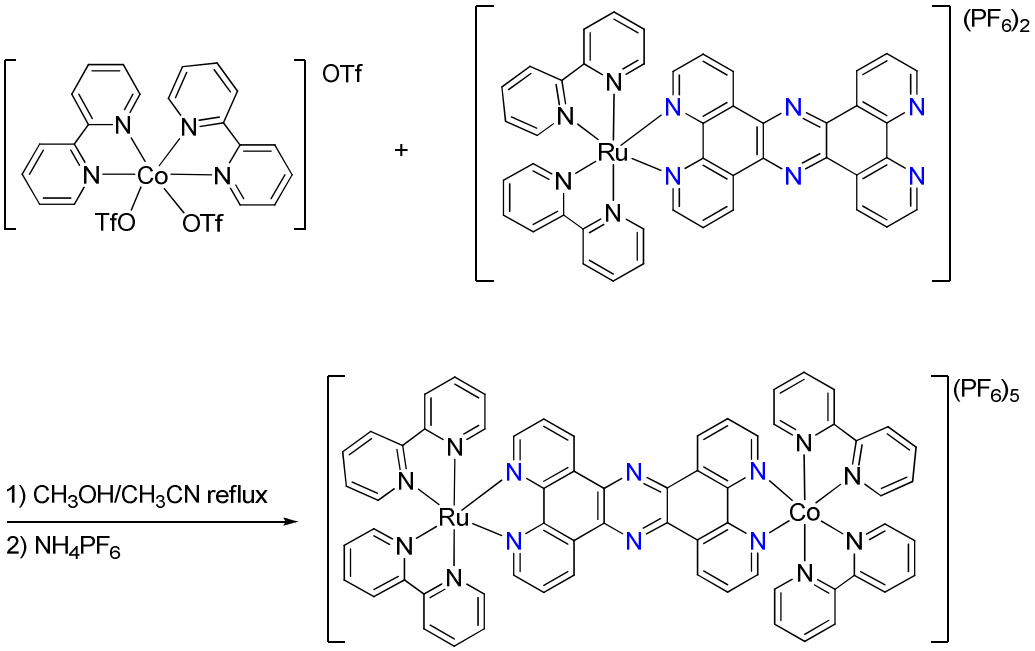

Procedure: In a 100 mL round-bottomed flask, (300 mg, 0.28 mmol) of $[Ru(bpy)_2(tpphz)](PF_6)_2$[3] was dissolved in 40 mL acetonitrile:methanol (1:1 v/v), then *cis*-$[Co(bpy)_2(OTf)_2]OTf$ (350 mg, 0.42 mmol) was added. The mixture was heated to reflux for 2.5 hours, after the mixture was cooled to room temperature, 40 mL NH_4PF_6 aqueous solution (1.3 g/10 mL) was added, a red solid was obtained. It was separated, washed with water, methanol and dried under vacuum, and 398 mg (75%) of $[Ru(bpy)_2(tpphz)Co(bpy)_2](PF_6)_5$ was obtained: ^{1}H NMR (400Hz, DMSO-d_6): δ 10.4 (d, 2H), 10.12 (d, 2H), 9.13 (d, 2H), 9.09 (d, 2H), 8.79 (t, 2H), 8.56 (t, 2H), 8.37 (m, 4H), 8.26 (t, 2H), 8.16 (m, 4H), 7.97 (d, 2H), 7.92 (t, 2H), 7.85 (d, 2H), 7.80 (t, 2H), 7.66 (q, 4H), 7.53 (d, 2H), 7.44 (m, 4H); HRMS for calculated for $C_{64}H_{54}N_{12}O_5F_{30}P_5CoRu\cdot H_2O$ 1604.1174 [M - $2PF_6$], found 1604.1230; Anal. Calcd for $C_{64}H_{54}N_{12}O_5F_{30}P_5CoRu\cdot H_2O$: C, 40.20; H, 2.80; N, 10.33. Found: C, 40.16; H, 2.42, N, 10.25.

References

1. Gosh, S.; Barve, A. C.; Kumbhar, A. A.; Kumbhar, A. S.; Puranik, V. G.; Datar, P. A.; Sonawane, U. B.; Joshi, R. R. *J. Inorg. Biochem.*, **2006**, 100, 331.
2. Bolinger, C. M.; Story, N.; Sullivan, B. P.; Meyer, T. J. *Inorg. Chem*. **1988**, *27*, 4582.
3. Bolger, J.; Gourdon, A.; Ishow, E.; Launay, J.-P.. *Inorg. Chem*. **1996** *35*, 2937.

^{1}H NMR spetcrum of $[Ru(bpy)_2tpphzCo(bpy)_2](PF_6)_5$ in DMSO-d_6.

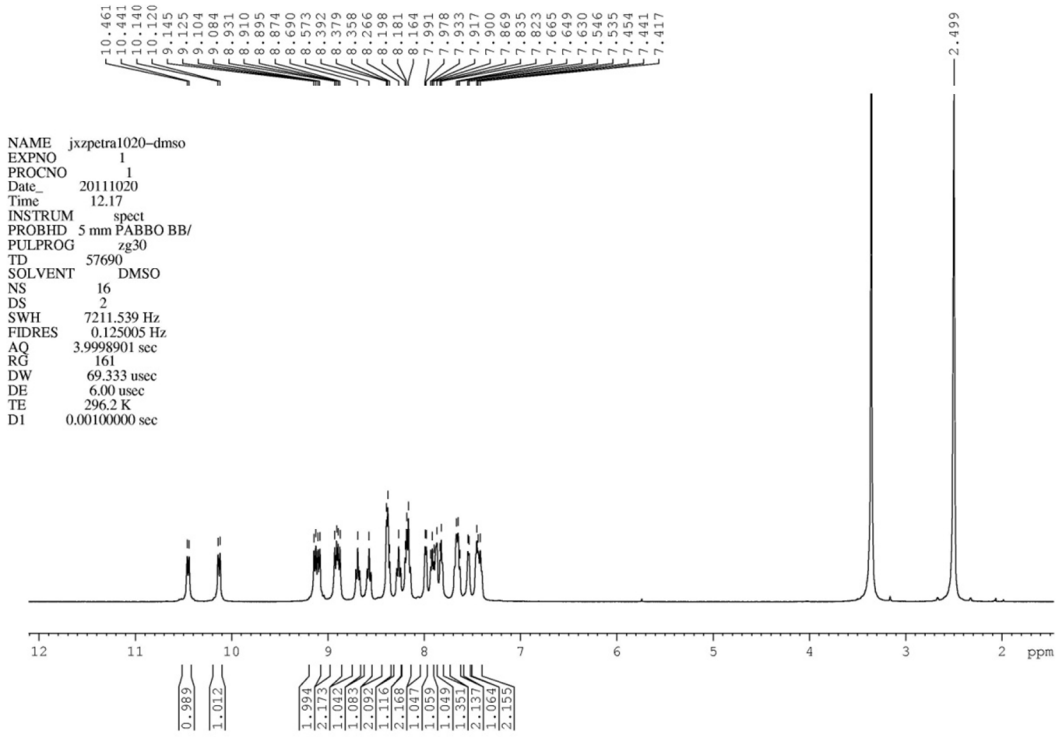

S_2 Cyclic voltammetry and spectroelectrochemistry.

Cyclic voltammetry

Cyclic voltammetry was carried out in a conventional three electrode configuration cell using a glassy carbon disc working electrode (d = 3 mm) and a Pt gauge as counter electrode. A non-aqueous Silver/Silver Ion (Ag/Ag^+) quasi-reference electrode (QRE, silver wire, 0.01M $AgNO_3$, 0.1M Bu_4NPF_6in acetonitrile) was used. A solution of 0.1M Bu_4NPF_6 in acetonitrile was used as electrolyte. About 10 mg of each sample was dissolved in 50 ml of electrolyte. Cyclic voltammetry was tested within the electrolyte window potential at 50 mV/ s. All electrochemical experiments were performed at room temperature. Oxidation and reduction of $[(bpy)_2Ru^{II}(tpphz)]^{3+}$ and $[(bpy)_2Ru^{II}(tpphz)^1Co^{III}(bpy)_2]^{5+}$ (abbreviated as $Ru^{II}=^1Co^{III}$ were fully reversible. The redox values are given in Table $S_{2\text{-}1}$. At the end of the experimental run, a reference voltammogram of Ferrocene was taken as internal standard. Its redox peak was located at 90.2 mV vs silver/silver ion (Ag/Ag^+) reference electrode.

	Ru Potential vs QRE	Co Potential vs QRE
Ferrocene	0.0902	
$[(bpy)_2Ru^{II}(tpphz)]^{3+}$	0.9345	
$[(bpy)_2Ru^{II}(tpphz)^1Co^{III}(bpy)_2]^{5+}$	1.0204	0.0864

Table $S_{2\text{-}1}$: Redox potentials, where QRE: Ag/ Ag^+ and E (vs QRE) + 0.542V= E (vs NHE).

Spectroelectrochemistry

With the redox potentials obtained from cyclic voltametry measurements, it was possible to acquire the UV-vis spectra of the oxidized and reduced $[(bpy)_2Ru^{II}(tpphz)^1Co^{III}(bpy)_2]^{5+}$. These species are abbreviated as $Ru^{III}=^1Co^{III}$ and $Ru^{II}=^4Co^{II}$ respectively in Figure $S_{2\text{-}2}$. The isosbestic point between $Ru^{II}=^1Co^{III}$ and $Ru^{III}=^1Co^{III}$ used in the transient optical measurements is clearly observed in the inset at 580 nm.

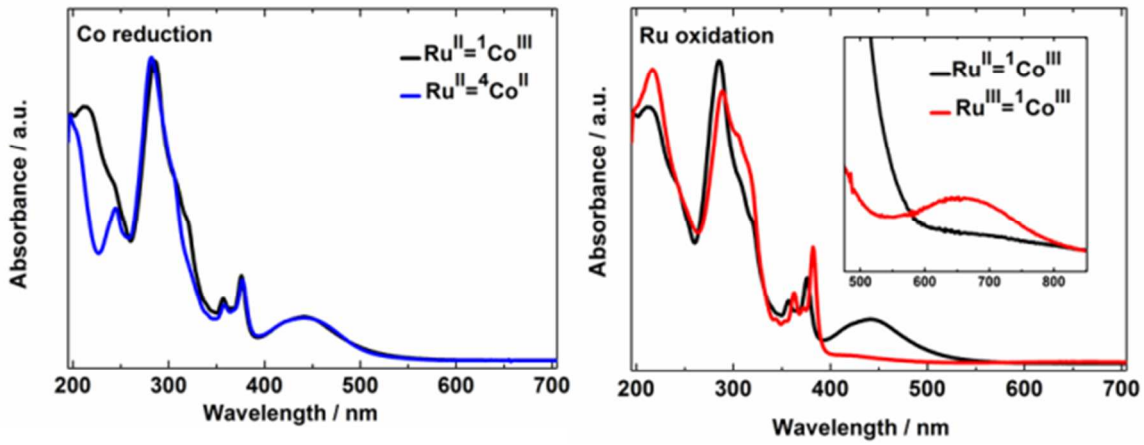

Figure $S_{2\text{-}2}$ UV-vis spectra of $Ru^{II}=^1Co^{III}$ (black), $Ru^{III}=^1Co^{III}$ (red) and $Ru^{II}=^4Co^{II}$ (blue) in acetonitrile.

S_3 Time-resolved optical spectroscopy.

The femtosecond laser setup is based on a Mai Tai pumped Spitfire Pro XP (Spectra Physics) with central output wavelength of 795 nm and 1 kHz repetition rate delivering ~80 fs pulses. The beam was split into two parts: one for pumping a collinear optical parametric amplifier (TOPAS-C, Light Conversion) to generate the pump beam, and the second one was either focused onto a 2-mm sapphire plate to generate a white light continuum (for transient spectra measurements), or was used for pumping a second TOPAS-C to generate narrow-band probe pulses (for kinetics measurements). The acquired probe beam was then led through a computer-controlled delay line. Subsequently, the probe pulses were split into two parts: the former overlapping with the pump pulse in the sample volume and the latter serving as a reference. The probe and the reference beams were then brought to the slit of a spectrograph and dispersed onto a double photodiode array, each with 512 elements (Pascher Instruments). The intensity of excitation pulses was kept below ~ 10^{14} photons per pulse per cm^2. Absorption spectra were measured before and after experiments to check for possible sample degradation, none was observed. The mutual polarization between pump and probe beams was set to the magic angle (54.7°) by placing a Berek compensator in the pump beam.

S_4 Time-resolved X-ray absorption (XA) spectroscopy set up at 11-ID-D of the Advanced Photon Source (APS) .

The time-resolved XA spectroscopy measurements were carried out at beamline 11-ID-D of the APS (Argonne National Laboratory). The optical pump pulse consisted of the second harmonic output of a Nd:YLF regenerative amplified laser at 1.6 kHz repetition rate, giving 527 nm laser pulses with 5 ps FWHM. The X-ray probe pulses with 79 ps FWHM and 6.5 MHz repetition rate were derived from the electron bunches stored in the APS ring. $[(bpy)_2Ru^{II}(tpphz)^1Co^{III}(bpy)_2]^{5+}$ (abbreviated as $[Ru^{II}=^1Co^{III}]$) was dissolved in acetonitrile to reach 1.7 mM. This concentration ensured that the signal was not distorted by self-absorption effects (see X-ray detection below). The liquid sample was flowed through a stainless steel tube and formed a free jet of 550 μm in diameter inside an air-tight Aluminum chamber. The sample was degassed by bubbling Nitrogen. Laser and X-ray beams were overlapped spatially on the replenishing sample. The time delay between the laser and X-ray pulses was fixed by a programmable delay line (PDL-100A-20NS, Colby Instruments) that adjusted the phase shift of the mode-lock driver for the seed laser relative to that of the RF signal of the storage ring with a precision of 500 fs. The incident X-ray energy was stepped through the Co K edge (7709 eV) up to 700 eV above the 1s threshold. A Co metal foil placed between two conventional ionization chambers downstream was used for X-ray energy calibration purpose in transmission mode. Two avalanche photodiodes (APDs) were positioned at 90˚ angle on both sides of the incident X-ray beam to collect the emitted X-ray fluorescence signals. A [Soller slits/(Z-1) Fe filter] combination, which was custom-designed for the specific sample chamber configuration and the distance between the sample and the detector, was inserted between the sample jet and the APD detectors. This greatly reduced the background due X-ray elastic scattering. An additional APD was employed to monitor the intensity of the incident X-ray beam. The outputs of the APDs were sent to two fast analyzer cards (Agilent) that were triggered by a signal at 1.6 kHz from the scattered laser light onto a photo diode. The card digitized the X-ray fluorescence signals as a function of time at 1ns/point after each trigger. The fluorescence signals from the synchronized X-ray pulse at 3 ns delay after the laser pump pulse excitation were accumulated to build the XA trace μ (laser-on). The fluorescence signals from the same X-ray pulse averaged over 50 round trips in the storage ring prior to the laser pulse were averaged to build the corresponding XA trace μ (laser-off). With this collection scheme, the (laser-on) and (laser-off) data were taken under the exact same detection conditions for sample, laser and beamline, with the shot-to-shot normalization of the X-ray pulse intensities performed by the acquisition software. This allowed cancelling out any error associated to drifts. Analyzing the difference signal $\Delta\mu = [\mu(laser\ on) - \mu(laser\ off)]$ originating from the fraction α of molecules in the excited state delivers the XA spectrum of the photoinduced species $[Ru^{III}=^4Co^{II}]$. The integrity of the sample over time was checked by comparing from scan to scan the lineshapes of the (laser-off) trace. For Co^{III} complexes, The XANES region is known to be particularly sensitive to any radiation damage. No change could be detected throughout the duration of the experiment.

S_5 Computational details and results for the DFT calculations on $^1Co^{III}(bpy)_3$(LS) and $^4Co^{II}(bpy)_3$ (HS).

All calculations were carried out with the ORCA program package.[r1] The geometries of $^1Co^{III}(bpy)_3$ (LS, S=0) and $^4Co^{II}(bpy)_3$ (HS, S=3/2) were fully optimized with the B3LYP*/TZVP method. This functional has provided reasonable results for the structures and energetics of the LS and HS states of transition metal complexes.[r2] These DFT-optimized structures were used in the FEFF 9.0 simulations that guided interpretation of the transient X-ray absorption spectra described in this work. The cartesian coordinates are given below.

References:

(r1) Neese, F. *ORCA*, version 2.8; Max-Planck-Institut fu□r Bioanorganische Chemie: Mu□lheim an der Ruhr, Germany, 2004.
(r2) (a) Paulsen, H; Trautwein, A. X. *Top. Curr. Chem.* **2004**, *235*, 197-219. (b) Hauser, A. *Coord. Chem. Rev.* **2006**, *250*, 1642-1652. (c) Vargas, A.; Zerara, M.; Krausz, E.; Hauser, A.; Daku, L. M. L. *J. Chem. Theory Comput.* **2006**, *2*, 1342-1359. (d) Shiota, Y.; Sato, D.; Juhász, G.; Yoshizawa, K. *J. Phys. Chem. A* **2010**, *114*, 5862-5869. (e) Pápai, M.; Vankó, G.; de Graaf, C.; Rozgonyi, T. *J. Chem. Theory Comput.* Article ASAP, **DOI**: 10.1021/ct300932n.

$^1Co^{III}(bpy)_3$ (LS, S=0)

```
61
Coordinates from ORCA-job Co3-bipy-LS-opt-B3LYPx-TZVP
  H       2.778049      2.358179      3.606511
  H       2.190967      4.652845      2.769776
  C       2.125283      2.496378      2.752174
  C       1.795447      3.765269      2.287828
  H      -3.428218      1.218318      3.612766
  H       0.648527     -3.586662      3.603535
  H       1.832595      0.388259      2.446453
  H       2.927920     -4.226454      2.765861
  C       1.599241      1.387013      2.105262
  C      -3.221746      0.587592      2.755712
  H      -1.251386      1.393437      2.449410
  C       0.951268      3.880969      1.189077
  H       0.686802      4.861254      0.812817
  C       1.095182     -3.089017      2.750687
  H      -5.122262     -0.433245      2.770201
  C       2.358270     -3.438170      2.285073
  C      -1.998985      0.691011      2.107463
  H      -0.583055     -1.778721      2.445436
  C      -4.156157     -0.329634      2.287571
  C       0.397822     -2.076790      2.105107
  N       0.779715      1.496125      1.044158
  C       0.450726      2.732368      0.579778
  C       2.881507     -2.763281      1.187529
  H       3.861930     -3.025874      0.811075
  N       0.902557     -1.419979      1.045240
```

N	-1.683513	-0.070302	1.044735
C	-3.834166	-1.114447	1.186548
C	2.137277	-1.753692	0.579819
H	-0.686799	4.861255	-0.812820
C	-0.450725	2.732368	-0.579779
H	-4.551361	-1.831817	0.807371
C	-2.589093	-0.972353	0.578177
C	-0.951265	3.880969	-1.189078
C	2.589093	-0.972352	-0.578177
H	4.551360	-1.831817	-0.807371
N	-0.779715	1.496125	-1.044157
N	1.683513	-0.070301	-1.044734
C	3.834166	-1.114446	-1.186548
C	-2.137277	-1.753692	-0.579819
C	-1.795445	3.765269	-2.287829
N	-0.902557	-1.419979	-1.045240
C	1.998985	0.691012	-2.107462
H	-2.190965	4.652844	-2.769778
C	4.156156	-0.329633	-2.287571
H	1.251386	1.393440	-2.449408
C	-1.599242	1.387013	-2.105261
C	3.221746	0.587594	-2.755710
H	-3.861931	-3.025874	-0.811075
H	5.122262	-0.433244	-2.770201
C	-2.881507	-2.763281	-1.187530
C	-2.125284	2.496377	-2.752173
H	-1.832597	0.388259	-2.446451
H	3.428219	1.218320	-3.612764
C	-0.397823	-2.076789	-2.105107
H	0.583055	-1.778719	-2.445436
H	-2.778050	2.358178	-3.606510
C	-2.358270	-3.438169	-2.285073
C	-1.095182	-3.089016	-2.750688
H	-2.927921	-4.226452	-2.765861
H	-0.648527	-3.586661	-3.603536
Co	-0.000000	0.002832	0.000000

$^{4}Co^{II}(bpy)_3$ (HS, S=3/2)

61
Coordinates from ORCA-job Co2-bipy-HS-opt-B3LYPx-TZVP

H	3.874044	0.544829	-3.539891
H	5.245613	-1.355297	-2.637433
C	3.536153	-0.041555	-2.693685
C	4.291669	-1.095593	-2.192248
H	-1.366344	-3.641309	-3.578940
H	-2.345246	3.072443	-3.606860
H	1.704445	1.064939	-2.438056
H	-1.429303	5.216342	-2.675070
C	2.324875	0.249440	-2.082177

C	-1.727407	-3.054620	-2.742549
H	0.121962	-1.979871	-2.476233
C	3.810053	-1.813646	-1.104862
H	4.394333	-2.631534	-0.703867
C	-1.683685	3.076475	-2.748633
H	-3.697927	-3.929011	-2.692752
C	-1.171244	4.261043	-2.231698
C	-0.895471	-2.126462	-2.131341
H	-1.707787	0.935041	-2.501524
C	-3.018776	-3.207742	-2.251171
C	-1.327687	1.882551	-2.136392
N	1.850495	-0.443659	-1.037242
C	2.578239	-1.471466	-0.542476
C	-0.326533	4.207221	-1.130085
H	0.067952	5.125211	-0.714935
N	-0.507428	1.822437	-1.077381
N	-1.286061	-1.366030	-1.099138
C	-3.428850	-2.426839	-1.178355
C	0.000104	2.969659	-0.570840
H	3.511929	-3.709823	0.814984
C	1.988093	-2.189408	0.616247
H	-4.428306	-2.547603	-0.781627
C	-2.544321	-1.500998	-0.621000
C	2.581494	-3.312839	1.197947
C	0.900649	2.823296	0.600320
H	1.500532	4.893646	0.757176
N	0.819745	-1.696460	1.089404
N	1.027514	1.572811	1.100550
C	1.590721	3.896584	1.168241
C	-2.907969	-0.622405	0.517951
C	1.967456	-3.929991	2.281217
N	-1.908140	0.126433	1.036138
C	1.821411	1.371583	2.162364
H	2.419810	-4.801980	2.740111
C	2.407160	3.681333	2.271389
H	1.888505	0.351444	2.523837
C	0.230245	-2.301528	2.131371
C	2.525242	2.393941	2.783253
H	-5.005844	-1.134291	0.609497
H	2.945107	4.508439	2.721173
C	-4.202658	-0.549080	1.037455
C	0.767027	-3.417141	2.760593
H	-0.704566	-1.869065	2.469111
H	3.148919	2.181252	3.643492
C	-2.169732	0.938551	2.070645
H	-1.333769	1.517450	2.447093
H	0.254601	-3.867356	3.602300
C	-4.464686	0.289872	2.113005
C	-3.428513	1.048792	2.645158
H	-5.465730	0.352232	2.525610
H	-3.587440	1.714702	3.485063
Co	-0.000253	0.003855	0.00284

S_6 Procedure for fitting the difference XA spectrum.

The general methodology for extracting photoinduced structural changes by fitting directly the transient difference XA spectrum $\Delta\mu = [\mu(laser\ on) - \mu(laser\ off)]$ has been presented in (1, 2, 3). For the [Ru^{II}=$^1Co^{III}$] complex under study, the excited state fraction α of [Ru^{III}=$^4Co^{II}$] formed through electron transfer was first determined independently by minimizing the difference $D = \sum_1^N \frac{1}{\sigma_i^2}(\Delta\mu(i) - \alpha \times Ref(i))^2$, where N is the number of data points, σ_i are the variance estimated from the experimental error bars and *Ref* is the reference trace constructed from the mononuclear complexes (see main text). A value of 65 ± 3 % was found for α. The Co-N distance noted R was taken as the sole varying structural parameter. A molecular editor was used to generate the x, y, z coordinates of geometries with bond length elongations of $\Delta R_i = i \times 0.01$ Å. FEFF 9.0 (3,4) calculations of the EXAFS profile for the DFT optimized ground state of $[^1Co^{III}(bpy)_3]^{2+}$ (see SI_5) were performed to adjust the non-structural parameters to match the experimental [Ru^{II}=$^1Co^{III}$] spectrum. The simulations of the profiles for each of the molecules with a Co coordination sphere expanded by ΔR_i were then run, giving traces Sim_i. The experimental and simulated profiles were interpolated on a grid equally-spaced in k, as for steady-state EXAFS data collection, although no FFT was later on applied. This ensured that the spectra of the references, the $\mu(laser\ off)$ and the reconstructed excited state could be processed using the conventional EXAFS softwares (4) Athena and Artemis (see (4) and S_7 below). The pseudo chi-squared function $chi_2 = \sum_2^9 \frac{k^2}{\sigma_k^2}(\Delta\mu(k) - \alpha \times Sim_i(k))^2$ was calculated and plotted as a function of ΔR_i in Figure $S_{6\text{-}1}$. It is minimum for $\Delta R_i = 0.20$ Å.

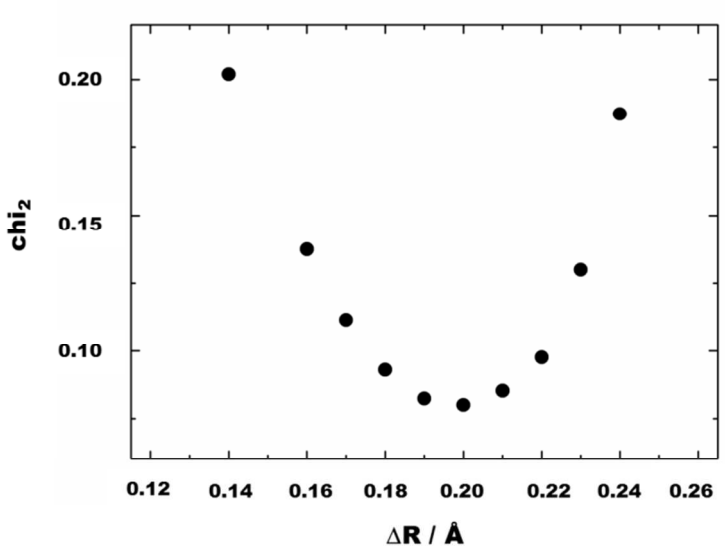

Figure $S_{6\text{-}1}$ Function chi_2 as function of the bond elongation ΔR_i

The statistically-correct estimation of all the variances from the experimental error bars is not straightforward and had to be omitted at this stage of the analysis. This awaits for benchmarking very systematically and carefully the combined influence of, not only the detection systems on the time resolved setup, but also the effect of sampling and resampling schemes in E and k space necessarily introduced for fitting. Such work is currently in progress. Nevertheless, renormalizing the chi_2 values to

the minimum value reached for $\Delta R_i = 0.20$ Å allows using this indicator as a conventional chi-square estimate (7). The value for which $chi_2 = 2$ are the limits of the 1-σ confidence interval, resulting in $\Delta R_i = 0.20$ Å $\pm$ 0.03 Å.

References

1. Smolentsev, G.; Soldatov, A.V. J. Synchrotron Radiat. **2006**, 13, 19.
2. Smolentsev, G.; Soldatov, A.V. Comput. Mater. Sci. **2007**, 39, 569.
3. http://www.nano.sfedu.ru/fitit.html
4. http://cars9.uchicago.edu/ifeffit/
5. Ankudinov, A.L.; Ravel, B.; Rehr, J.J.; Conradson, S.D. Phys. Rev. B **1998**, 58, 7565.
6. http://leonardo.phys.washington.edu/feff
7. Sunhong Jun, S.; Lee, J.H.; J.; Kim, J.; Kim, J.; Kim, K.H.; Kong, Q.Y.; Kim, T.K.; Lo Russo, M.; Wulff, M.; Ihee, H. Phys. Chem. Chem. Phys. **2010**, 12, 11536.

S_7 Reconstructed excited state spectrum.

With a reliable 65+/-3% excited state fraction estimated from the scaling of the normalized transient signal $\Delta\mu$ to the reference trace, it is possible to reconstruct the XA spectrum of the $[Ru^{III}=^4Co^{II}]^{5+}$ HS species. It is shown in Fig $S_{7\text{-}1}$ (red) and compared to the reference complex $[^4Co^{II}(bpy)_3]^{2+}$HS (gray).

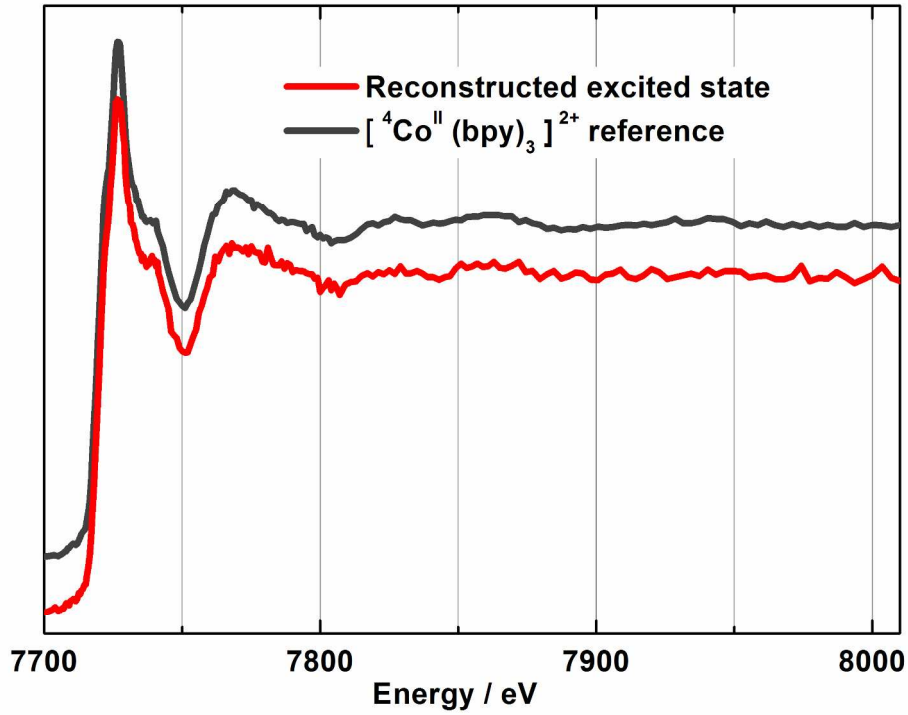

Figure $S_{7\text{-}1}$ Reconstructed excited state spectrum with a 65% excited state fraction (red) compared with the $^4Co^{II}(bpy)_3]^{2+}$ HS reference (gray).

S_8 Fitting of the X-ray kinetics recorded at 7720 eV.

The X-ray kinetics trace taken at 7720 eV monitors the decay of the $[^4Co^{II}(bpy)_3]^{2+}$ HS species (Fig 4. in the main text). It can be fitted with a single exponential function convoluted with a gaussian of 40 ps FWHM that accounts for the temporal width of the X-ray beam. The time constant obtained is 45 +/- 2 ns, with 95% confidence limit.